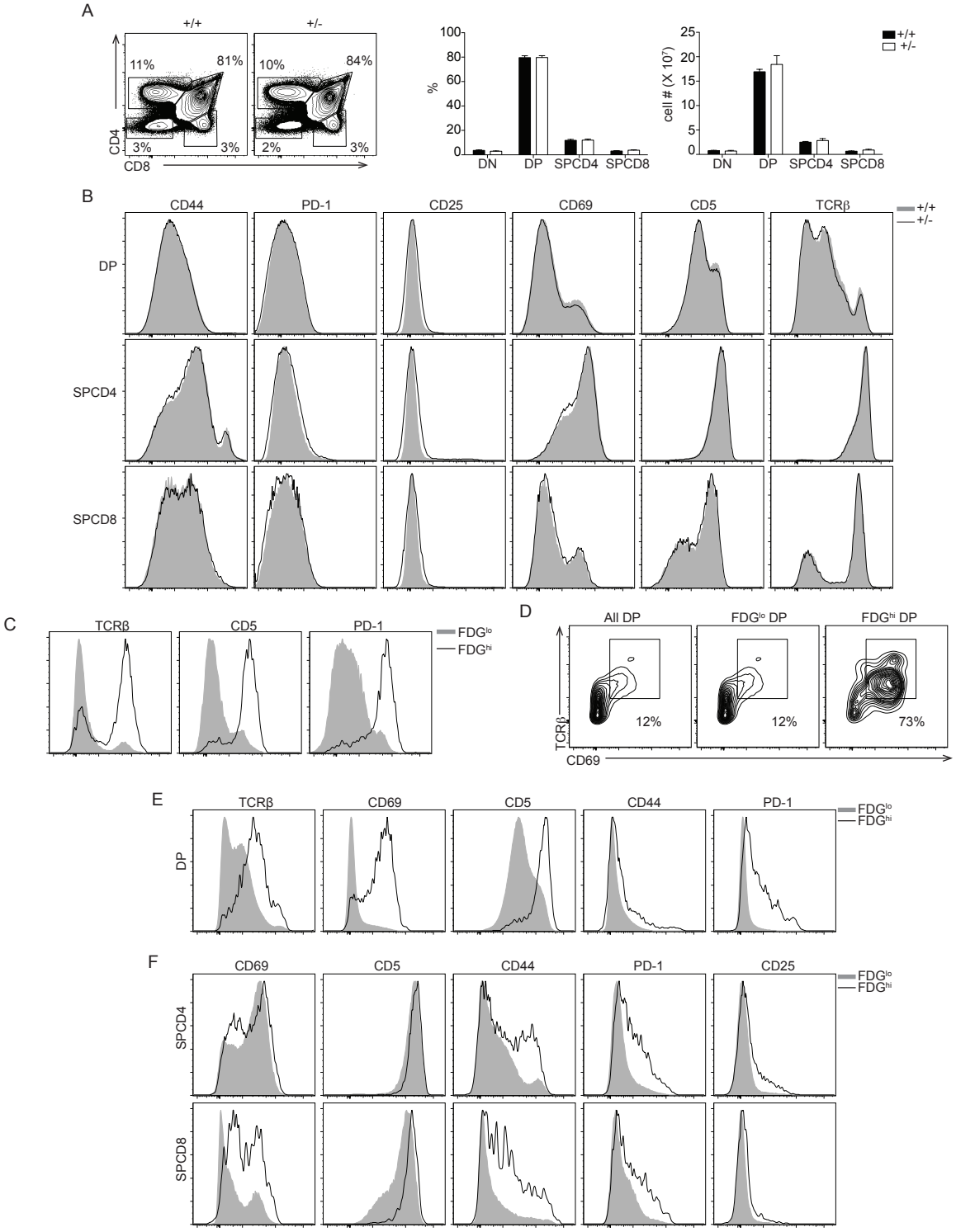

Supplemental Figure 1: Phenotype of *Nr4a3*$^{+/-}$ mice used for FDG expression studies and additional FDG-expression data. (**A**) Distribution and phenotype (**B**) of the main thymocyte populations found in *Nr4a3*$^{+/+}$ and *Nr4a3*$^{+/-}$ mice. (**C**) FDG^{hi} DN thymocytes express TCRβ, CD5 and PD-1. The β-galacosidase substrate FDG was used as a surrogate marker for *Nr4a3* expression in CD4^{-}CD8^{-} DN thymocytes of *Nr4a3*$^{+/-}$ mice. (**D-F**) FDG expression was measured by flow cytometry in thymocytes from *Nr4a3*$^{-/-}$ mice. (**D**) The profile of TCRβ and CD69 expression for total DP (left), FDG^{lo} DP (middle) and FDG^{hi} DP (right) in *Nr4a3*$^{-/-}$ mice. The percentage of post-selection DP (TCRβ^{hi}CD69^{hi}) for each subset is shown. Representative histograms of the indicated markers among FDG^{lo} and FDG^{hi} DP (**E**) or SP (**F**) thymocytes from *Nr4a3*$^{-/-}$ mice.

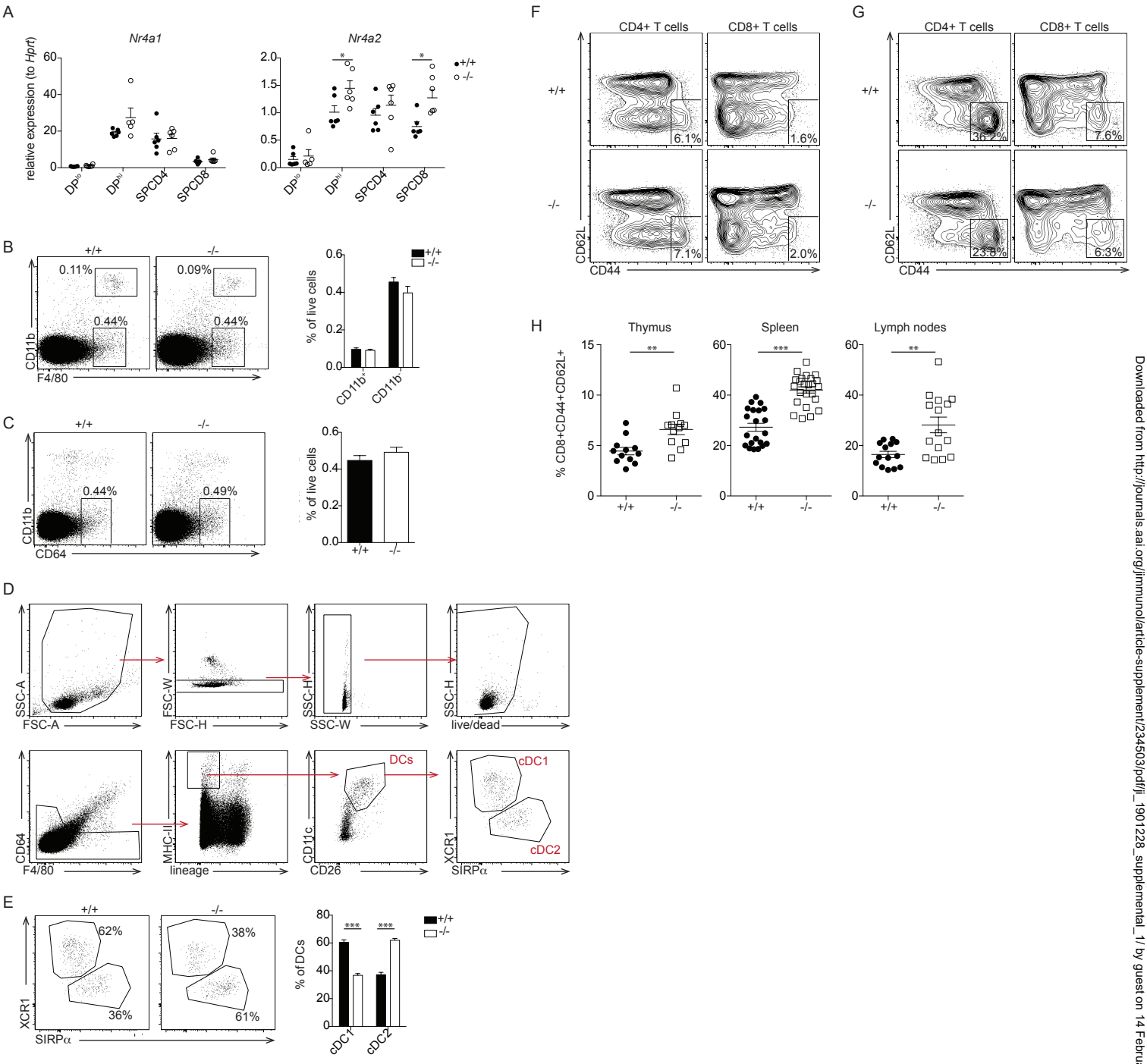

Supplemental Figure 2: Impact of *Nr4a3*-deletion on thymocyte *Nr4a1* and *Nr4a2* transcription, macrophage and DC populations and peripheral T cells. (**A**) qRT-PCR analysis of *Nr4a1* and *Nr4a2* transcription in sorted thymocyte populations. (**B**) Thymuses from *Nr4a3*$^{+/+}$ and *Nr4a3*$^{-/-}$ were analyzed for the distribution of CD11b^{+}F4/80^{+} and CD11b^{-}F4/80^{+} macrophages. (**C**) Alternate gating strategy to indentify CD11b^{-} macrophages. (**D**) Gating strategy to idendify thymic cDC1 and cDC2 populations. The lineage panel includes anti-CD19, -B220, -NK1.1 and -CD3 (**E**) Proportion of cDC1 and cDC2 in the thymus of *Nr4a3*$^{+/+}$ and *Nr4a3*$^{-/-}$ mice. T cells from (**F**) lymph nodes and (**G**) spleens of *Nr4a3*$^{+/+}$ and *Nr4a3*$^{-/-}$ mice were characterized for CD44 and CD62L expression. (**H**) Compilation of the percentage of CD8^{+}CD62L^{+}CD44^{+} cells found in the thymus, spleen and lymph nodes of *Nr4a3*$^{+/+}$ and *Nr4a3*$^{-/-}$ mice. For (B-C and E), 10 (+/+) and 7 (-/-) mice per group from 3 independent experiments. Contour plots in (F-G) are shown for 12 week-old mice.

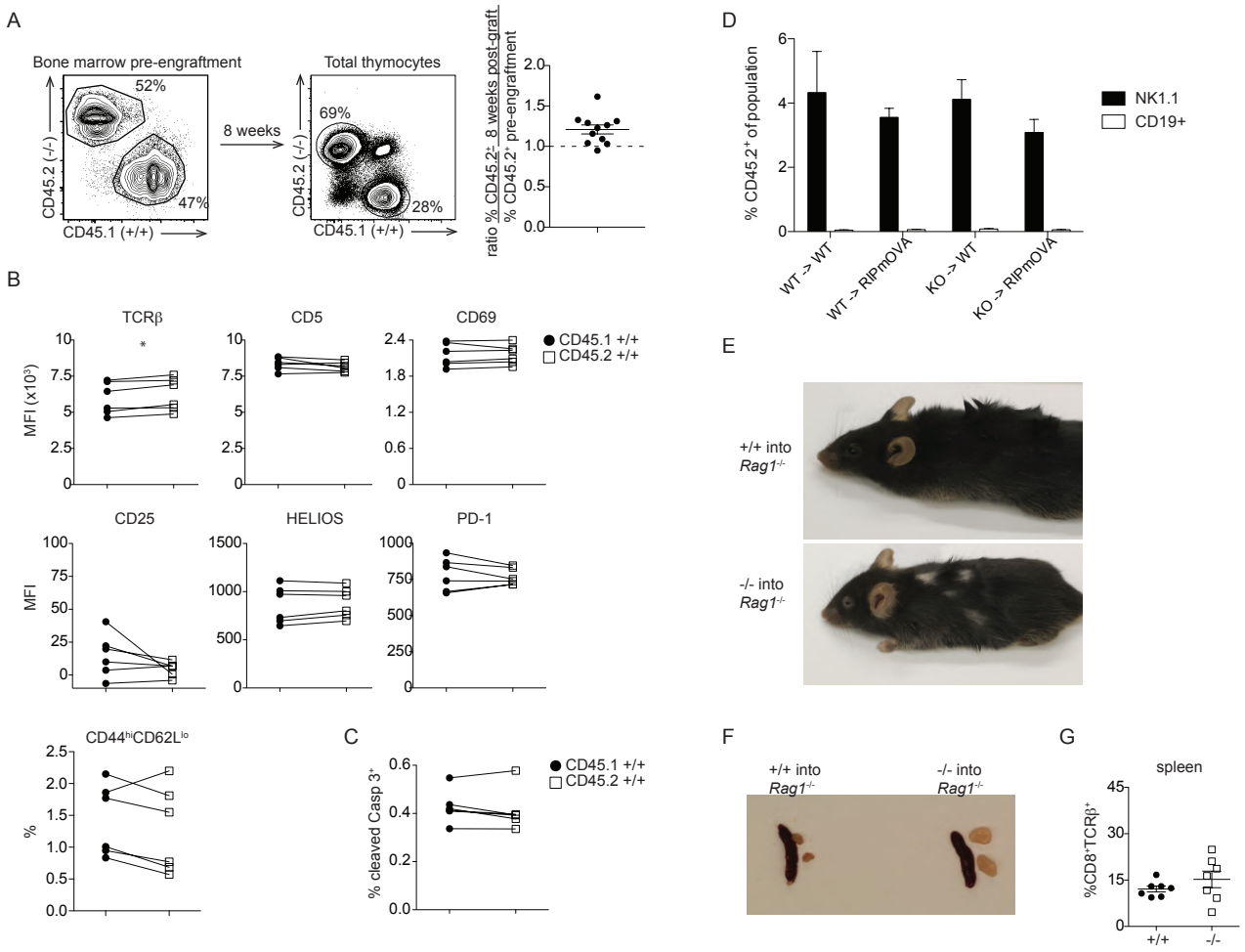

Supplemental Figure 3: *Nr4a3*$^{-/-}$ controls for mixed bone marrow chimeras and no overt phenotype in WT:WT chimeras. (**A**) Bone marrow cells from CD45.1^{+} *Nr4a3*$^{+/+}$ mice were mixed with those from CD45.2 *Nr4a3*$^{-/-}$ mice. These cells were injected in lethally irradiated CD45.1.2^{+} recipients. 8 weeks later, proportion of CD45.1^{+} and CD45.2^{+} thymocytes were analyzed by flow cytometry. (**B-C**) Bone marrow cells from CD45.1^{+} *Nr4a3*$^{+/+}$ mice were mixed at a 1:1 ratio with those from CD45.2 *Nr4a3*$^{+/+}$ mice. These cells were injected in lethally irradiated CD45.1.2^{+} recipients. 8 weeks later, the phenotype of SPCD8 thymocytes (**B**) and the proportion of TCRβ^{+}CD5^{+}active Caspase3^{+} of CD45.1^{+} and CD45.2^{+} thymocytes was compared (**C**). (**D**) Controls for RIP-mOVA chimeras. Wild-type or RIP-mOVA recipients were grafted with a mixture of 3% *Nr4a3*$^{+/+}$ or *Nr4a3*$^{-/-}$ OT-I bone marrow cells (CD45.2^{+}) and CD45.1^{+} B6.SJL cells. 6-weeks post-irradiation, the proportion of splenic OT-I-derived (*Nr4a3*$^{+/+}$ or *Nr4a3*$^{-/-}$) CD45.2^{+} NK1.1^{+} or CD19^{+} cells was measured by flow cytometry (**E-G**) Adoptive transfer of *Nr4a3*$^{-/-}$ SPCD8 thymocytes into *Rag1*$^{-/-}$ mice can cause observable skin irritation. RAG1-deficient mice were adoptively transferred with 1 x 10^{6} sorted SPCD8 thymocytes from *Nr4a3*$^{+/+}$ or *Nr4a3*$^{-/-}$ mice. At least 30 days later, mice were euthanized and skin irratation was visible in some recipeint mice (**E**). (**F**) Spleen an skin draining lymph nodes from these recipient mice. (**G**) Number of CD8^{+} T cells found in the spleen of *Rag1*$^{-/-}$ recipients.

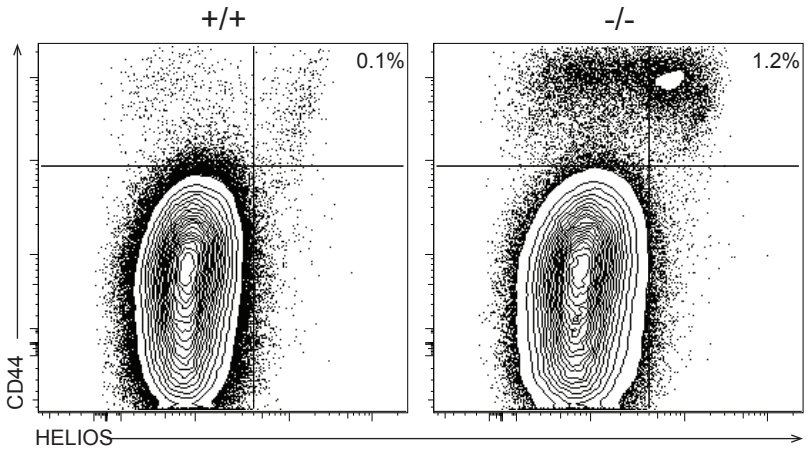

Supplemental Figure 4: CD44^{hi}HELIOS^{+} activated thymocytes are detected at the DP stage in *Nr4a3*$^{-/-}$ mice. DP thymocytes from *Nr4a3*$^{+/+}$ and *Nr4a3*$^{-/-}$ mice were stained for CD44 and HELIOS.